



Analysis of a propagating crack tip in orthotropic functionally graded materials



Kwang Ho Lee*

Department of Automotive Engineering, Kyungpook National University, Sangju City, Kyeongbuk, 742-711, South Korea

ARTICLE INFO

Article history:

Received 15 December 2014

Received in revised form

8 August 2015

Accepted 22 August 2015

Available online 3 September 2015

Keywords:

B. Anisotropy

B. Fracture

C. Analytical modelling

Functionally graded materials (FGMs)

Orthotropic FGMs (OFGMs)

ABSTRACT

Crack tip stress and displacement fields for a propagating crack at constant velocity along a gradient in orthotropic functionally graded materials (OFGMs) with an exponential variation of the shear modulus and density are developed. The crack tip fields are obtained by using wave potentials and the Airy stress function through an asymptotic analysis. Solutions are obtained for orthotropic characteristics of two kinds. Using the stress fields, the effects of material nonhomogeneity on the stress components are investigated. In addition, contours of the constant maximum shear stress at a propagating crack tip are generated and the effects of material nonhomogeneity on the isochromatics are discussed.

© 2015 Published by Elsevier Ltd.

1. Introduction

In light of the recent development of various functionally graded materials (FGMs), it is important to evaluate their integrity. Thus, many researchers have studied the fracture behavior of nonhomogeneous materials. Despite theoretical, numerical and experimental works having been conducted on the static or propagating cracks in FGMs, the dynamic fractures of orthotropic FGMs (OFGMs) have rarely been studied. Specially, the study on propagating crack tip fields has not been reported.

The behaviors of propagating cracks in FGMs have attracted much research attention. Propagating cracks in FGMs were first studied by Atkinson and List [1,2]. Since then, several groups [3–5] have investigated the behavior of cracks in FGMs. Jiang and Wang [6] developed the opening and sliding displacements for a propagating crack in an FGM in which the properties were assumed to vary exponentially perpendicular to the crack propagation direction. Meguid et al. [7] performed a theoretical analysis of a finite crack propagating in an infinite inhomogeneous medium. Ma et al. [8] analyzed crack propagation in a functionally graded strip under plane loading. Lee et al. [9] developed nonhomogeneity-specific

terms for stress and displacement fields by using displacement potentials under thermo-mechanical loading. Lee [10] developed the crack tip fields for a propagating crack in FGMs with property variation angled to the crack direction by using displacement potentials. Lee [11] also developed a transiently propagating crack in FGMs under a mixed mode. These crack tip solutions of Lee were obtained by transforming the general partial differential equations of the dynamic equilibrium into Laplace's equations whose solutions have harmonic functions. Thus, the fields can be expressed very simply. In experimental studies on FGMs, Orat and Lambros [12] studied the fracture at crack initiation under the mixed mode state. Tilbrook et al. [13] studied the influence on crack propagation trajectory with Moiré interferometry in FGM under mode I loading. Yao et al. [14] studied the fracture with caustic experiment when a crack propagates along the elastic gradient in an FGM under mode I loading. Liu et al. [15] presented the numerical results in buckling failure analysis of cracked FGM under uniaxial and biaxial compression loads.

In all these studies, fracture analysis was conducted on cracks in FGMs. With regard to crack in OFGMs, for static crack, Amada and Untao [16] studied fracture properties of bamboo which is natural OFGM. Dag et al. [17] performed static fracture analysis of OFGMs numerically under mechanical and thermal loading, and Chalivendra [18] obtained static fields by asymptotic analysis with the Wastergaard stress function. Bayesteh and Mohammadi [19]

* Tel.: +82 54 530 1404.

E-mail address: khl@knu.ac.kr.

performed static fracture analysis of OFGMs using the extended finite element method (XFEM). Wang et al. [20] obtained elasticity solutions for orthotropic functionally graded curved beam. For propagating crack, Ma et al. [21] studied the stress intensity factors for a moving Griffith crack (Yoffe type crack) in OFGMs in which the properties were assumed to vary exponentially perpendicular to the crack propagation direction. Lee et al. [22] analyzed the stress and displacement fields for a propagating mode III crack tip in OFGMs. However, the stress and displacement fields at propagating mode I and II crack tip in OFGMs have not yet been reported. Such stress and displacement fields are required in the analysis of full field experimental data obtained through techniques such as photoelasticity and caustics or in the analysis of numerical data as finite element method and boundary element method.

Thus, the present study develops the stress and displacement fields for a crack propagating at uniform speed along the direction of property variation in an FGM under inplane loading. The shear modulus and density of the FGM are assumed to vary exponentially along the gradation direction. The elastodynamic problem for OFGMs is formulated in terms of displacement potentials and the solution is obtained through an asymptotic analysis. The effects of material nonhomogeneity on stress components are studied using the stress fields developed in this study. Furthermore, the effects of material nonhomogeneity on the isochromatics for a propagating crack in FGMs are discussed.

2. Stress and displacement fields for OFGMs

2.1. Formulation of dilatational and shear wave potentials

The orthotropic elastic constants C_{ij} and density ρ of an OFGM under a constant Poisson's ratio ν are assumed to vary exponentially as given in Eq. (1).

$$C_{ij} = C_{ij}^0 \exp(\zeta X), \quad \rho = \rho_0 \exp(\zeta_d X) \quad (1)$$

where C_{ij}^0 and ρ_0 are material constants and the density at $\mathbf{X} = 0$ respectively. ζ and ζ_d are the nonhomogeneity parameters of shear modulus and density respectively. When the angle (α) between the elastic principal (reinforcement) direction and the crack direction is $\alpha = 0^\circ$ or $\alpha = 90^\circ$ as shown in Fig. 1, the relationship between stresses and strains can be written as

$$\begin{aligned} \sigma_{XX} &= e^{\zeta X} [C_{11}^0 \varepsilon_{XX} + C_{12}^0 \varepsilon_{YY}] \\ \sigma_{YY} &= e^{\zeta X} [C_{21}^0 \varepsilon_{XX} + C_{22}^0 \varepsilon_{YY}] \\ \tau_{XY} &= e^{\zeta X} C_{66}^0 \gamma_{XY} \end{aligned} \quad (2)$$

where σ_{ij} and ε_{ij} are the inplane stress and strain components respectively. C_{ij}^0 values differ according to the plane stress and plane

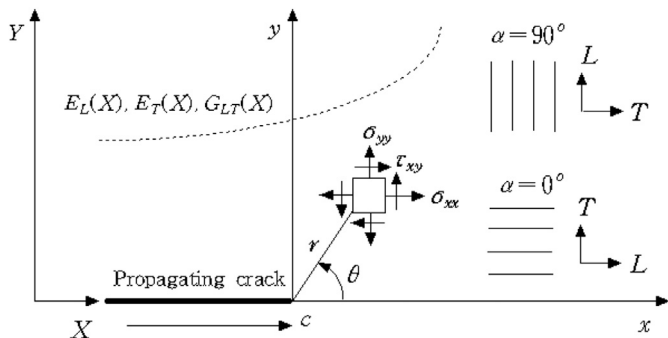


Fig. 1. Stress components at crack tip in OFGM.

strain states. If $\alpha \neq 0^\circ$ or $\alpha \neq 90^\circ$, the physical property at the crack tip is an anisotropic state and C_{16} and C_{26} are present in the inplane.

The displacements \mathbf{u} and \mathbf{v} that are derived from the dilatational and shear wave potentials Φ and Ψ can be expressed by Eq. (3)

$$\mathbf{u} = \frac{\partial \Phi}{\partial X} + \frac{\partial \Psi}{\partial Y}, \quad \mathbf{v} = \frac{\partial \Phi}{\partial Y} - \frac{\partial \Psi}{\partial X} \quad (3)$$

The equilibrium in the dynamic state is given by Eq. (4)

$$\frac{\partial \sigma_X}{\partial X} + \frac{\partial \tau_{XY}}{\partial Y} = \rho \frac{\partial^2 \mathbf{u}}{\partial t^2}, \quad \frac{\partial \tau_{XY}}{\partial X} + \frac{\partial \sigma_Y}{\partial Y} = \rho \frac{\partial^2 \mathbf{v}}{\partial t^2} \quad (4)$$

Substituting of Eqs. (1) and (2) into Eq. (3), and Eq. (3) into Eq. (4), the equations for the dynamic state can be obtained as

$$\begin{aligned} e^{\zeta X} \left[C_{11}^0 \left(\frac{\partial^3 \Phi}{\partial X^3} + \frac{\partial^3 \Psi}{\partial X^2 \partial Y} \right) + C_{12}^0 \left(\frac{\partial^3 \Phi}{\partial X \partial Y^2} - \frac{\partial^3 \Psi}{\partial X^2 \partial Y} \right) \right. \\ \left. + C_{66}^0 \left(2 \frac{\partial^3 \Phi}{\partial X \partial Y^2} + \frac{\partial^3 \Psi}{\partial Y^3} - \frac{\partial^3 \Psi}{\partial X^2 \partial Y} \right) \right] + \zeta e^{\zeta X} \left[C_{11}^0 \left(\frac{\partial^2 \Phi}{\partial X^2} + \frac{\partial^2 \Psi}{\partial X \partial Y} \right) \right. \\ \left. + C_{12}^0 \left(\frac{\partial^2 \Phi}{\partial Y^2} - \frac{\partial^2 \Psi}{\partial X \partial Y} \right) \right] = \rho_0 e^{\zeta_d X} \frac{\partial^2}{\partial t^2} \left(\frac{\partial \Phi}{\partial X} + \frac{\partial \Psi}{\partial Y} \right) \end{aligned} \quad (5-a)$$

$$\begin{aligned} e^{\zeta X} \left[C_{22}^0 \left(\frac{\partial^3 \Phi}{\partial Y^3} - \frac{\partial^3 \Psi}{\partial X \partial Y^2} \right) + C_{21}^0 \left(\frac{\partial^3 \Phi}{\partial X^2 \partial Y} + \frac{\partial^3 \Psi}{\partial X \partial Y^2} \right) \right. \\ \left. + C_{66}^0 \left(2 \frac{\partial^3 \Phi}{\partial X^2 \partial Y} - \frac{\partial^3 \Psi}{\partial X^3} + \frac{\partial^3 \Psi}{\partial X \partial Y^2} \right) \right] \\ \left. + \zeta e^{\zeta X} C_{66}^0 \left(2 \frac{\partial^2 \Phi}{\partial X \partial Y} - \frac{\partial^2 \Psi}{\partial X^2} + \frac{\partial^2 \Psi}{\partial Y^2} \right) \right] = \rho_0 e^{\zeta_d X} \frac{\partial^2}{\partial t^2} \left(\frac{\partial \Phi}{\partial Y} - \frac{\partial \Psi}{\partial X} \right) \end{aligned} \quad (5-b)$$

For a propagating crack along X -axis in fixed coordinates (X, Y) , the transformed crack tip coordinates (x, y) are $\mathbf{x} = \mathbf{X} - \mathbf{ct}$, $\mathbf{y} = \mathbf{Y}$, where c is a constant crack tip speed and t is time. When a complex variable is given as $z = x + my$, where m is a dependant variable on physical properties, nonhomogeneity and crack speed, Eq. (5) around the crack tip can be expressed as

$$\begin{aligned} \alpha_1(m) \frac{\partial^3 \Phi(z)}{\partial z^3} + \beta_1(m) \frac{\partial^3 \Psi(z)}{\partial z^3} + \zeta \left[(C_{11}^0 + C_{12}^0 m^2) \frac{\partial^2 \Phi}{\partial z^2} \right. \\ \left. + m(C_{11}^0 - C_{12}^0) \frac{\partial^2 \Psi}{\partial z^2} \right] = 0 \end{aligned} \quad (6-a)$$

$$\begin{aligned} \alpha_2(m) \frac{\partial^3 \Phi(z)}{\partial z^3} + \beta_2(m) \frac{\partial^3 \Psi(z)}{\partial z^3} + \zeta \left[2mC_{66}^0 \frac{\partial^2 \Phi}{\partial z^2} \right. \\ \left. + C_{66}^0 (m^2 - 1) \frac{\partial^2 \Psi}{\partial z^2} \right] = 0 \end{aligned} \quad (6-b)$$

where

$$\alpha_1(m) = (C_{12}^0 + 2C_{66}^0)m^2 + C_{11}^0 - \rho_0 c^2 e^{(\zeta_d - \zeta)X}$$

$$\beta_1(m) = m \left[C_{66}^0 m^2 + (C_{11}^0 - C_{12}^0 - C_{66}^0 - \rho_0 c^2 e^{(\zeta_d - \zeta)X}) \right]$$

$$\alpha_2(m) = m \left[C_{22}^0 m^2 + (C_{12}^0 + 2C_{66}^0 - \rho_0 c^2 e^{(\zeta_d - \zeta)X}) \right]$$

$$\beta_2(m) = (C_{12}^0 + C_{66}^0 - C_{22}^0)m^2 - C_{66}^0 + \rho_0 c^2 e^{(\zeta_d - \zeta)X}$$

Download English Version:

<https://daneshyari.com/en/article/7213019>

Download Persian Version:

<https://daneshyari.com/article/7213019>

[Daneshyari.com](https://daneshyari.com)